TÜBİTAK

Turkish Journal of Chemistry

http://journals.tubitak.gov.tr/chem/

Research Article

Turk J Chem
(2014) 38: 775 – 782

doi:10.3906/kim-1312-28

Graphene oxide–magnetite nanocomposite as an efficient and magnetically separable adsorbent for methylene blue removal from aqueous solution

Kadem MERAL, Önder METİN*
Department of Chemistry, Faculty of Science, Atatürk University, Erzurum, Turkey

Received: 11.12.2013 • **Accepted:** 17.02.2014 • **Published Online:** 15.08.2014 • **Printed:** 12.09.2014

Abstract: We report a facile method to produce a magnetically separable graphene oxide–magnetite nanocomposite (GO–Fe_3O_4) and its adsorption performance in methylene blue (MB) removal from aqueous solution. The GO–Fe_3O_4 nanocomposite was synthesized by a solution-phase self-assembly method including the incorporation of monodisperse Fe_3O_4 nanoparticles (NPs) and GO in a dimethylformamide/chloroform mixture under sonication. The successfully decorating GO sheet with monodisperse Fe_3O_4 NPs was proved by TEM study. ICP–OES data of the GO–Fe_3O_4 nanocomposite show that the GO–Fe_3O_4 nanocomposite consists of 21 wt% Fe_3O_4 NPs, which is sufficient for its magnetic separation from aqueous solution. The spectroscopic studies reveal that the GO–Fe_3O_4 nanocomposite is a highly efficient adsorbent for MB removal from aqueous solution, providing an adsorption capacity of 172.6 mg/g, and the equilibrium for MB adsorption is attained in ∼70 min. Moreover, it is a magnetically separable and reusable material for MB removal from water, preserving 87% of its initial efficiency after 5 successive runs.

Key words: Graphene oxide, Fe_3O_4 nanoparticles, composite sorbent, magnetic separation, dye removal, methylene blue

1. Introduction

Organic dye compounds are widely used in many important industries such as textile, plastics, paint, leather, and cosmetics.[1] Therefore, significant amounts of those dyes are discharged as colored effluents into the environment during the product purification steps.[2] In this regard, the removal of organic dyes from wastewater has become a significant issue with the increasing concern about environmental protection.[3,4] Various techniques such as adsorption,[5] flocculation,[6] oxidation,[7] biological treatment,[8] and photocatalysis[9] have been employed to eliminate organic dyes from industrial wastewaters. However, the adsorption method is the most convenient one considering its efficiency, practicability, and low cost.[10,11]

Activated carbons are the most commonly used adsorbents for organic dye removal,[12] but their high costs and the difficulty in recycling them hinder their larger scale application.[13] Therefore, cheaper and more effective adsorbents instead of activated carbons are needed for organic dye removal from industrial effluents. Recently, graphene has emerged as a versatile material for various applications owing to its unique physical and chemical properties.[14] Although graphene has a huge surface area, its application in organic dye removal from effluents is not practicable due to its limited dispersion in water and difficulty in its synthesis on a large scale. However, graphene oxide (GO) represents a very appropriate platform for many applications owing to its

*Correspondence: ometin@atauni.edu.tr

hydroxyl, epoxy, and carboxylic acid groups enabling its high dispersion in water.[15] Therefore, GO can be used as a highly efficient adsorbent in organic dye removal from water.[16,17] However, the separation of suspended GO from water is rather difficult after the adsorption process, which forms an important obstacle preventing its practical use in industry.

It is well known that magnetic separation provides important advantages such as being a rapid and effective way for removing and recycling magnetic particles or composites by applying an external magnet.[18] Magnetite (Fe_3O_4) nanoparticles (NPs) are one of the most important superparamagnetic materials due to their high saturation magnetization and low toxicity.[19] Fe_3O_4 NPs can be synthesized in various sizes and morphologies and used in many technological applications.[20,21] For this reason, the GO–Fe_3O_4 nanocomposite, which combines the adsorption properties of GO along with the merit of easy separation due to the incorporation of magnetic NPs, could be a very efficient adsorbent for dye removal from aqueous solutions. GO–Fe_3O_4 nanocomposites are generally synthesized by the in situ reduction of water-soluble iron salts into GO nanosheets. However, the carboxylic, epoxy, and hydroxyl groups of GO were mostly lost during the in situ reduction processes, resulting in a poor dispersion of the nanocomposite in water or other polar solvents. Moreover, the in situ methods lack the size control, metal content, and nanoparticle morphology on GO. In this regard, the synthesis of Fe_3O_4 NPs via organic solution phase synthesis with a controlled size and morphology in one step and then their controlled loading on GO nanosheets via liquid-phase self-assembly method would be a promising way for the preparation of highly efficient nanocomposites for organic dye removal from aqueous solution and many technological applications.

In the present study, a facile method for the preparation of a magnetically separable GO–Fe_3O_4 nanocomposite and its satisfactory performance in methylene blue (MB) removal from aqueous solution was developed. The GO–Fe_3O_4 nanocomposite was synthesized by a solution-phase self-assembly method including the incorporation of monodisperse Fe_3O_4 NPs[22] and GO in a dimethylformamide/chloroform mixture under sonication.[23] The GO–Fe_3O_4 nanocomposite was characterized by using various advanced analytical techniques. The efficiency of the GO–Fe_3O_4 nanocomposite for MB removal from aqueous solution was studied by UV-Vis spectroscopy depending on the effect of contact time and initial MB concentration. The spectroscopic studies revealed that the GO–Fe_3O_4 nanocomposite is a highly efficient and reusable adsorbent for MB removal from aqueous solution.

2. Result and discussion

2.1. Synthesis and characterization of the GO–Fe_3O_4 nanocomposite

The synthesis of monodisperse Fe_3O_4 NPs was done according to a well-established protocol in the literature[26] that includes the high temperature organic solution decomposition of $Fe(acac)_3$ by using OAm as both surfactant and reducing agent and BE as high-boiling-point solvent. Although the characterization of monodisperse Fe_3O_4 NPs and GO as well as GO–Fe_3O_4 nanocomposites was reported in the literature and/or our previous report,[22] we think that the presentation of some crucial ones here will be useful because we made some minor modifications to the synthesis protocols. Figure 1a shows a representative TEM image of Fe_3O_4 NPs that depicts the very narrow size distribution of them with a mean particle size of 8 nm. A representative TEM image of GO nanosheets is given by Figure 1b that depicts the transparent and very thin layered structure of GO clearly. Next, monodisperse Fe_3O_4 NPs were deposited into GO nanosheets by using a solution phase self-assembly method in a DMF/chloroform mixture. Figure 1c shows a TEM image of the GO–Fe_3O_4 nanocomposite in which the good dispersion of Fe_3O_4 NPs on thin-layered GO by preserving their size and morphology can be

seen. Next, the magnetic properties of the GO–Fe_3O_4 nanocomposite were studied by magnetic hysteresis at room temperature and are depicted in Figure 1d. The GO–Fe_3O_4 nanocomposite has a specific saturation magnetization (Ms = 18.2 emu g^{-1}) with a typical superparamagnetic hysteresis loop. Comparing this value with the one obtained for Fe_3O_4 NPs (Ms = 56 emu g^{-1}), the lower Ms value of the GO–Fe_3O_4 stems from the low Fe_3O_4 NPs content (21 wt% Fe_3O_4 by ICP–OES analysis). However, this loading is sufficient for the easy removal of GO–Fe_3O_4 nanocomposite from the solution via a magnet.

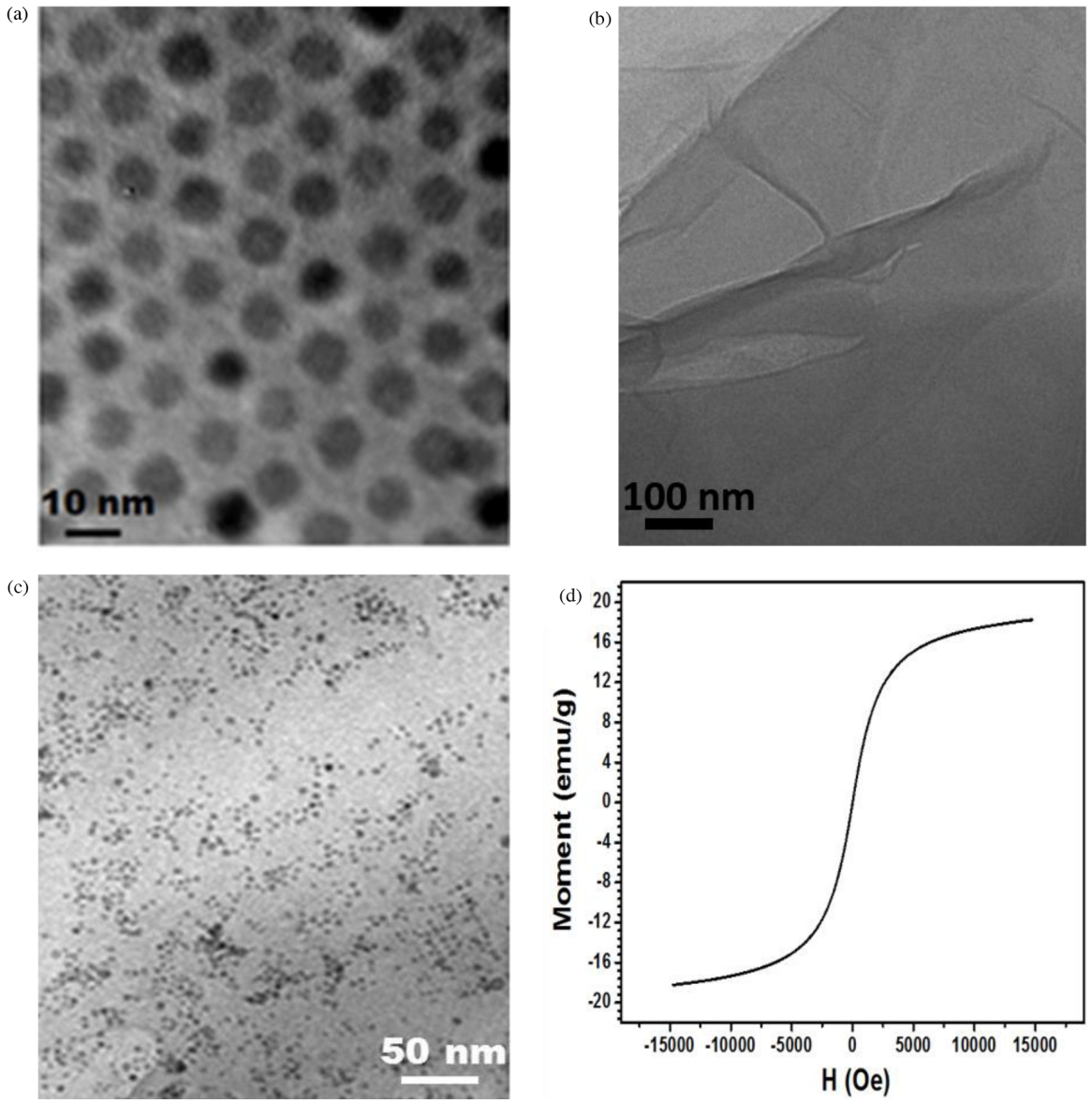

Figure 1. A representative TEM image of (A) as-prepared Fe_3O_4 NPs, (B) graphene oxide nanosheets, (C) GO–Fe_3O_4 nanocomposite, and (D) magnetic hysteresis loops of GO–Fe_3O_4 nanocomposite.

2.2. MB adsorption studies

The adsorption property of the GO–Fe_3O_4 nanocomposite was tested in the removal of MB from aqueous solution. Firstly, the effect of contact time on the amount of dye adsorbed was investigated at room temperature

(Figure 2). In order to determine the effect of contact time on the adsorption activity of the GO–Fe_3O_4 nanocomposite more accurately, 13 mg/L of aqueous MB solution was used for different contact time adsorption experiments. Dye aggregation was observed at high MB concentrations, which leads to deviation from Lambert–Beer's law. The spectroscopic results on time-dependent dye adsorption revealed that it took ~70 min for MB adsorption by the GO–Fe_3O_4 to reach equilibrium. The short equilibrium time shows that the GO–Fe_3O_4 nanocomposite possesses high adsorption efficiency to remove dye from aqueous solution. Additionally, it was observed that the dye removing efficiency of the GO–Fe_3O_4 nanocomposite was initially fast but then slower due to the decrease in the dye concentration. Moreover, the GO–Fe_3O_4 nanocomposite was easily separated from the dye solution by using an external magnet (inset of Figure 2). Figure 3 shows the adsorption isotherm of MB in the presence of the GO–Fe_3O_4 nanocomposite, which reveals the relationship between the amount of GO–Fe_3O_4 adsorbed per unit weight of the dye (qe, mg/g) and the concentrations of dye in the bulk solution (Ce, mg/L) under equilibrium conditions. The maximum adsorption capacity of MB in the concentration range studied was calculated to be 172.6 mg/g, which is higher than those reported previously.[17] Additionally, this value of the GO–Fe_3O_4 nanocomposite is satisfactory for MB when compared with the other several adsorbents reported so far (Table). We think that the electrostatic interaction between negatively charged GO sheets and cationic MB molecules as well as $\pi - \pi$ interaction induce the successful adsorption of MB on the GO–Fe_3O_4 nanocomposite. The pH effect on MB removal efficiency of the GO-Fe_3O_4 nanocomposite was evaluated at various pH values (pH 3 to 10). The efficiency of the GO–Fe_3O_4 nanocomposite is satisfactory in both acidic and alkaline media. However, the carboxylic acid and hydroxyl groups of GO are sensitive to pH alteration, which resulted in lower dispersion of GO–Fe_3O_4 nanocomposite in aqueous solution. Therefore, the removal efficiency of the GO–Fe_3O_4 nanocomposite is slightly decreased as a function of pH.

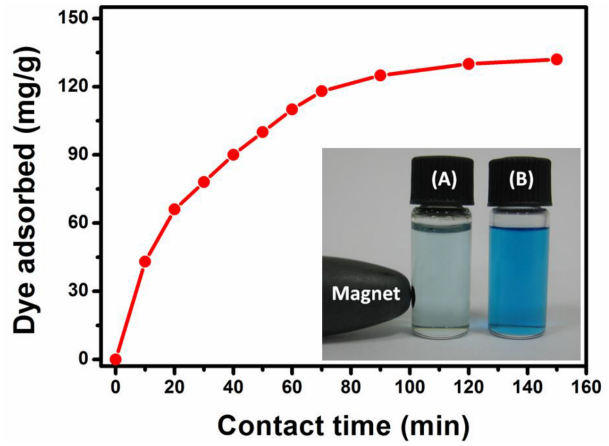

Figure 2. The effect of contact time on the MB adsorption of GO–Fe_3O_4 composite (the initial concentration of MB is 13 mg/L). The inset shows representative photos of MB solution for magnetic separation of the GO–Fe_3O_4 composite after dye adsorption (A) and before dye adsorption (B).

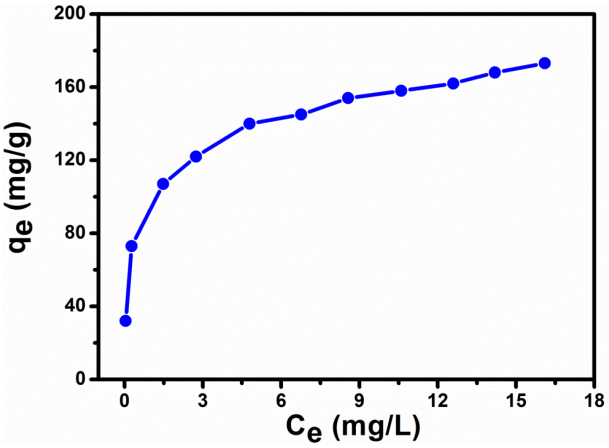

Figure 3. MB adsorption isotherm in the presence of the GO–Fe_3O_4 composite.

It is noteworthy that there were no changes observed in the morphology or structure of Fe_3O_4 NPs on GO sheets after the dye adsorption (Figure 4a), which reveals the stability of the GO–Fe_3O_4 nanocomposite in

aqueous solution. Moreover, the GO–Fe_3O_4 nanocomposite is magnetically recoverable and reusable for MB removal from aqueous solution. The reusability of the GO–Fe_3O_4 in MB removal was tested for 5 runs and the results are depicted in Figure 4b. Although the adsorption capacity of the GO–Fe_3O_4 nanocomposite for MB removal decreased a little for each successive run, it still had 87% of its initial efficiency after 5 successive runs.

Table. The adsorption capacity of various materials tested in MB removal.

Adsorbent	Adsorption capacity (mg MB/g)	Reference
GO–Fe_3O_4 hybrids	172.6	[this work]
MWCNTs with Fe_2O_3	42.3	[27]
Kaolinite	76.9	[28]
Na-ghassoulite	135	[29]
Activated carbon	521	[30]

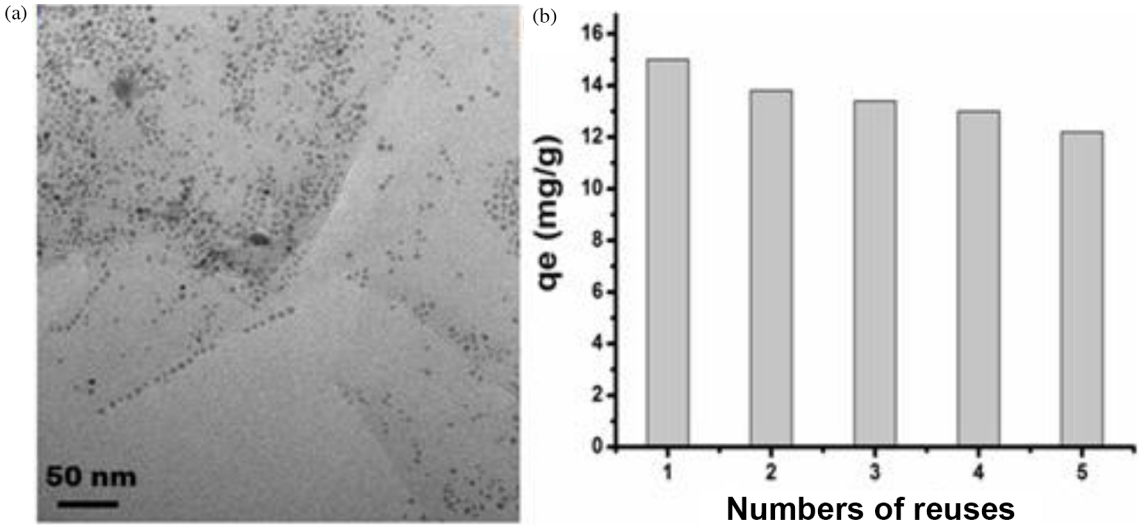

Figure 4. (A) TEM image of the GO–Fe_3O_4 hybrid composite after adsorption of MB, (B) the reusability of the GO–Fe_3O_4 composite in the MB removal from aqueous solution for 5 successive runs. ([GO–Fe_3O_4] = 0.6 g/L and [MB] = 13 mg/L).

In summary, the superparamagnetic GO–Fe_3O_4 nanocomposite synthesized with a solution phase self-assembly method was effectively used for dye removal from aqueous solution. The adsorbent ability of the GO–Fe_3O_4 nanocomposite was evaluated in MB removal from aqueous solution. Our spectroscopic studies revealed that the GO–Fe_3O_4 nanocomposite is highly efficient in removing of MB from aqueous solution and the adsorption capacity for MB dye in the concentration range studied is calculated to be 172.6 mg/g. The adsorption capacity value reported here is higher than those reported for GO–Fe_3O_4 nanocomposite prepared by in situ reduction method. The GO–Fe_3O_4 nanocomposite was easily separated by an external magnet from the dye solution after adsorption experiments, which provides a rapid and effective way for the separation of adsorbent from the solution. The GO–Fe_3O_4 nanocomposite showed high adsorption performance even after 5 cycles of dye removal, indicating its high durability and reusability in aqueous solution. Overall, we think that our GO–Fe_3O_4 nanocomposite has a great potential to be used as an adsorbent for organic dye removal from industrial wastewater as well as other applications such as catalysis.

3. Experimental section

3.1. Materials

Iron(III) acetylacetonate ($Fe(acac)_3$, ≥99.9%), oleylamine (OAm, >70%), benzyl ether (BE, 98%) potassium permanganate ($KMnO_4$, ≥99.9%), potassium peroxodisulfate ($K_2S_2O_8$, ≥99.9%), phosphorous pentaoxide (P_2O_5, ≥98%), hydrogen peroxide (H_2O_2, 30%), sodium nitrate ($NaNO_3$, ≥99.9%), sulfuric acid (H_2SO_4, 98%), N,N-dimethylformamide (DMF, 99.8%), and methylene blue (MB) were purchased from Sigma-Aldrich. Natural graphite flakes (average particle size 325 mesh) were purchased from Alfa Aesar. All chemicals were used without any further purification. Deionized water was distilled by water purification system (Milli-Q System).

3.2. Characterization

Transmission electron microscope (TEM) and high resolution TEM (HRTEM) images were obtained using a JEM-2100 (JEOL) instrument operating at 200 kV. The samples for TEM images were prepared by depositing the hexane dispersion of NPs on amorphous carbon-coated copper grids. Magnetic studies were performed on a Quantum Design Superconducting Quantum Interface Device (SQUID) with a field up to 70 kOe. UV-Vis spectroscopy analysis was performed on a PerkinElmer (model Lambda 35) spectrophotometer. Elemental analysis of the samples was done by using a Leiman series inductively coupled plasma-optical emission spectroscope (ICP-OES) after each sample was completely dissolved in aqua regia (HNO_3/HCl: 1/3 v/v ratio).

3.3. Synthesis of GO–Fe_3O_4 nanocomposite

The synthesis of the GO-Fe_3O_4 nanocomposite was done accordingly our procedure reported elsewhere with minor modifications.[22] In a typical recipe, the Fe_3O_4 NPs were synthesized via the organic solution phase synthesis starting from $Fe(acac)_3$ and using OAm as both surfactant and reducing agent and BE as solvent. In a separate step, GO nanosheets were synthesized by using the modified Hummers method.[24,25] Next, the Fe_3O_4 NPs were deposited on GO via a liquid self-assembly method to form GO–Fe_3O_4 nanocomposite.[22,23]

3.4. Adsorption experiments

The dye adsorption experiments were carried out in round bottom flasks at room temperature. In a typical experiment, 25 mL of aqueous solution of MB with a known initial concentration was mixed with 25 mg of the GO–Fe_3O_4 nanocomposite well-dispersed in water via sonication. The resultant mixture was shaken for 24 h at pH ∼5.8. Next, the GO–Fe_3O_4 nanocomposite was separated by an external magnet and the equilibrium concentrations of dye solutions were measured by a UV-Vis spectrophotometer at the maximum wavelength of absorption band of monomeric MB dye in water at 664 nm. The calibration curve was built for MB solutions in water at different concentrations. The amount of dye adsorbed was calculated using the following equation (Eq. (1)):

$$q_e = (C_o - C_e)V/m \tag{1}$$

where qe is the concentration of dye adsorbed (mg/g), C_o and C_e are the initial and equilibrium concentrations of dye (mg/L), m is the mass of the GO–Fe_3O_4 (g), and V is the volume of solution (L).[11,17] The adsorption experiment was also performed at different pH values by adjusting pH via use of HCl and NaOH.

3.5. Reusability experiment

To test the reusability of the GO–Fe_3O_4 nanocomposite for MB removal from water, 15 mg of the GO–Fe_3O_4 nanocomposite was added to 25 mL of MB dye solution (13 mg/L) and the mixture was stirred for 20 min at room temperature. After the separation of the nanocomposite via an external magnet, the supernatant dye solution was stored for the analysis of dye adsorption activity of the nanocomposite as described in the Adsorption experiments section. Then the MB adsorbed nanocomposite was washed with 25 mL of ethanol several times at room temperature. The GO–Fe_3O_4 nanocomposite was collected by an external magnet and reused for the second MB adsorption experiment. The reusability experiments were performed 5 times.

Acknowledgment

The financial support from Atatürk University Scientific Research Project Council (Project No: 2011/93) is gratefully acknowledged.

References

1. Chiou, M. S.; Ho, P. Y.; Li, H. Y. *Dyes & Pigments* **2004**, *60*, 69–84.
2. Sine, P. *Synthetic Dyes*, 1st ed. Rajat Publications: New Delhi, India, 2003.
3. Neill, C. O.; Hawkes, F. R.; Hawkes, D. L.; Lourenco, N. D.; Pinheiro, H. M.; Delee, W. *J. Chem. Tech. Biotechnol.* **1999**, *74*, 1009–1018.
4. Meunier, B. *Science* **2002**, *296*, 270–271.
5. Jiang, H.-L.; Tatsu, Y.; Lu, Z.-H.; Xu, Q. *J. Am. Chem. Soc.* **2010**, *132*, 5586–5587.
6. Zahrim, A. Y.; Tizaoui, C.; Hilal, N. *Desalination* **2011**, *266*, 1–16.
7. Serpone, N.; Horikoshi, S. A.; Emeline, V. *J. Photochem. Photobiol. C.* **2010**, *11*, 114–131.
8. Daneshvar, N.; Ayazloo, M.; Khataee, A. R.; Pourhassan, M. *Bioresource Technology* **2007**, *98*, 1176–1182.
9. Asl, S. K.; Sadrnezhaad, S. K.; Rad, M. K.; Uner, D. *Turk. J. Chem.* **2012**, *36*, 121–125.
10. Khan, M. A.; Lee, S. H.; Kang, S. *Sep. Sci. Technol.* **2011**, *46*, 1121–1130.
11. Crini, G. *Bioresource Technology* **2006**, *97*, 1061–1085.
12. Kannan, N.; Sundaram, M. M. *Dyes & Pigments* **2001**, *51*, 25–40.
13. Al-Degs, Y.; Khraished, M. A. M.; Allen, S. J.; Ahmad, M. N. A. *Sep. Sci. Technol.* **2001**, *36*, 91–102.
14. Geim, A. K. *Science* **2009**, *324*, 1530–1534.
15. Dreyer, D. R.; Park, S.; Bielawski, C. W.; Ruoff, R. S. *Chem. Soc. Rev.* **2010**, *39*, 228–240.
16. Liu, F.; Chung, S.; Oh, G.; Seo, T. S. *ACS Appl. Mater. Interfaces* **2012**, *4*, 922–927.
17. Xie, G.; Xi, P.; Liu, H.; Chen, F.; Huang, L.; Shi, Y.; Hou, F.; Zeng, Z.; Shao, C.; Wang, J. *J. Mater. Chem.* **2012**, *22*, 1033–1039.
18. Shylesh, S.; Schünemann, V., Thiel, W. R. *Angew. Chem. Int. Ed.* **2010**, *49*, 3428–3459.
19. Laurent, S.; Forge, D.; Port, M.; Roch, A.; Robic, C.; Elst, L. V.; Muller, R. N. *Chem. Rev.* **2008**, *108*, 2064–2110.
20. Çaldıran, Z.; Deniz, A. R.; Şahin, Y.; Metin, Ö.; Meral, K.; Aydoğan, Ş. *J. Alloy Compd.* **2013**, *552*, 437–442.
21. Karami, B.; Eskandari, K.; Ghasemi, A. *Turk. J. Chem.* **2012**, *36*, 601–614.
22. Metin, Ö.; Aydoğan, Ş.; Meral, K. *J. Alloy Compd.* **2014**, *585*, 681–688.
23. Gao, S.; Sun, S. *J. Am. Chem. Soc.* **2012**, *134*, 2492–2495.

24. Kovtyukhova, N. I.; Ollivier, P. J.; Martin, B. R.; Mallouk, T. E.; Chizhik, S. A.; Buzaneva, E. V.; Gorchinskiy, A. D. *Chem. Mater.* **1999**, *11*, 771–778.

25. Hummers, W. S.; Offeman, R. E. *J. Am. Chem. Soc.* **1958**, *80*, 1339–1339.

26. Sun, S.; Zeng, H. *J. Am. Chem. Soc.* **2002**, *124*, 8204–8205.

27. Qua, S.; Huanga, F.; Yua, S.; Chenc, G.; Kong, J. *J. Hazard. Mater.* **2008**, *160*, 643–647.

28. Ghosh, D.; Bhattacharyya, K. G. *Appl. Clay Sci.* **2002**, *20*, 295–300.

29. Mouzdahir, Y. E.; Elmchaouri, A.; Mahboub, R.; Gil, A.; Korili, S. A. *J. Chem. Eng. Data* **2007**, *52*, 1621–1625.

30. Juang, R.; Wu, F.; Tseng, R. *J. Colloid Interf. Sci.* **2000**, *227*, 437–444.